International Journal of Power Electronics and Drive Systems (IJPEDS)
Vol. 12, No. 3, September 2021, pp. 1586~1597
ISSN: 2088-8694, DOI: 10.11591/ijpeds.v12.i3.pp1586-1597

Implementation on the dSPACE 1104 of VOC-SVM based anti-windup PI Controller of a three-phase PWM rectifier

J. Lamterkati[1], L. Ouboubker[2], M. Khafallah[3], A. El afia[4]
[1]RITM Laboratory, Higher School of Technology, Casablanca (ESTC), Morocco
[1,2,3,4]Energy and Electrical Systems Laboratory, ENSEM, Hassan II University, Casablanca, Morocco
[2]LGEMS Laboratory, ENSA-Agadir, Ibn Zohr University, Agadir, Morocco
[4]ENSAM, Hassan II University, Casablanca, Morocco

Article Info

Article history:

Received Dec 29, 2020
Revised Jun 27, 2021
Accepted Jul 2, 2021

Keywords:

Anti-windup PI controller
dSPACE 1104
Space vector modulation
Three-phase PWM rectifier
Voltage oriented control

ABSTRACT

The study made in this paper concerns the use of the voltage-oriented control (VOC) of three-phase pulse width modulation (PWM) rectifier with constant switching frequency. This control method, called voltage-oriented control with space vector modulation (VOC-SVM). The proposed control scheme has been founded on the transformation between stationary (α-β) and and synchronously rotating (d-q) coordinate system, it is based on two cascaded control loops so that a fast inner loop controls the grid current and an external loop DC-link voltage, while the DC-bus voltage is maintained at the desired level and ansured the unity power factor operation. So, the stable state performance and robustness against the load's disturbance of PWM rectifiers are boths improved. The proposed scheme has been implemented and simulated in MATLAB/Simulink environment. The control system of the VOC-SVM strategy has been built based on dSPACE system with DS1104 controller board. The results obtained show the validity of the model and its control method. Compared with the conventional SPWM method, the VOC-SVM ensures high performance and fast transient response.

Corresponding Author:

Jawad Lamterkati
Departement of Electrical Engineering
Hassan II, University
Higher School of Technology (ESTC), Casablanca, Morocoo
Email: jawad.lamterkati@gmail.com

1. INTRODUCTION

The use of high-power electronics is being extended to different system related to power generation, industrial equipements, traction applications. Unfortunately, the standar diode/thyristor bridge rectifiers at the input side cause several problems as: Low power factor, high values of harmonic distortion of a line current and harmonic pollution on the grid, uncontrolled DC-link output voltage and the power flow unidirectionnel. So, new generation of controlled rectifiers has been investigated know as three-phase voltage source PWM rectifiers. The PWM rectifier is a preferred choise for providing a DC loads or voltage source fed drives, due to its capability of DC voltage control and bi-directional power flow, input power factor regulation, line current harmonic reduction [1], [2].

For improving the input power factor and shaping the input current into sinusoidal waveform, various control algorithms for PWM rectifier have been proposed in recent researchses which can be subdivised in to two groups according to their use of current control loop or active/reactive power control loop [3]-[9]: The voltage-oriented control (VOC), virtual flux-oriented control (VFOC), the voltage based

direct power control (V-DPC) and virtual flux based direct power control (VF-DPC). A wellknow algorithm among indirect power control that uses current controller is the method that is called voltage-oriented control (VOC), it's similar to the field-oriented control (FOC) of the induction motor, where the VOC method is able to produce high dynamic and static performance throuph the usage of internal current control loops and an outer voltage control loop. VOC is based on the rotating synchronous reference frame orientation with respect to the grid line voltage vector. By transforming the three phase quantities to appropriate DC components, the proportional and integral (PI) controllers are able to lead to estimated *dq* components to the desired reference values with zero steady state error [8]-[12]. The *d*-axis reference current is controlled to perform the DC-link voltage regulation while the reference current in *q*-axis is controlled to obtain a unity power factor [13].

Many different PWM modulation schemes are being used, such as sinusoidal PWM, delta modulation techniques and the space vecteur technique. It has been analyzed theorically and proved that the SVM technique is the best modulation solution on the whole. SVM is the best way to suppress the input harmonic as well for specific applications such as motor speed control. Another advantage of using SVM technique in inverter can achieve 15% more fundamental component in the output voltage and provides 33% reduction of effective switching frequency. However, switching losses also strongly depend on a load power factor. It is very important criterion, which allows farther reduction of switching losses up to 50% [14]. Finally, the proposed VOC-SVM technique was tested both in simulation and experimentally, using dSPACE 1104-based experimental prototype, and illustrative results are presented. Results confirm the effectiveness and the high performance of the proposed VOC.

2. WORKING PRINCIPLES AND MODELING OF THREE-PHASE PWM RECTIFIER

The circuit diagram of the three-phase voltage source rectifier structure is shown in Figure 1. In order to set up math model, it is assumed that the AC voltage is a balanced three-phase supply, the filter reactor is linear, IGBT is ideal switch and lossless [15], [16]. The converter is connected to the three-phase power supply via an inductor *L* and internal resistance *R* for each phase. The three-phase voltage supply is denoted e_a, e_b and e_c. Three identical line inductors indicated by L_a, L_b and L_c act as line filters for smoothing the line current with minimum ripples. Each inductor has an internal resistance which is denoted by R_a, R_b and R_c. A part of reducing the total harmonic distortion (THD) of the line currents, the inductions also provide the boost the feature of the converter. Six power transistors (IGBTs) with anti-parallel diode are used as the SVR power switches, since, IGBTs have features of high-power rating which is used to carry out the PWM generation as well as the power bidirectional conversion, a load and capacity are connected simultaneously at the output of the converter. The capacity is used as a voltage source and follows the rectifier to also operate as an inverter [17].

The state of switches in each of the leg can be described using switching function defined in (1).

$$S_k(t) = \{0,1\},\ k = a,b,c \tag{1}$$

There are six actives' states of converter for $Sa + Sb + Sc = \{1,2\}$ and two passive states for $Sa + Sb + Sc = \{0,3\}$. In each of the active state there exists a circuit for energy transfer between the DC and AC side.

The voltage equations are given by:

$$\begin{cases} e_a = L\frac{di_a}{dt} + Ri_a + v_a \\ e_b = L\frac{di_b}{dt} + Ri_b + v_b \\ e_c = L\frac{di_c}{dt} + Ri_c + v_c \end{cases} \tag{2}$$

The current across C is:

$$C\frac{dv_{dc}}{dt} = S_a i_a + S_b i_b + S_c i_c - i_L \tag{3}$$

The (2) can be rewritten as following:

$$\begin{cases} L\frac{di_d}{dt} = e_d - Ri_d + \omega Li_q - v_d \\ L\frac{di_q}{dt} = e_q - Ri_q - \omega Li_d - v_q \\ C\frac{dv_{dc}}{dt} = \frac{3}{2}\left(S_d i_d + S_q i_q\right) - \frac{v_{dc}}{R_L} \end{cases} \quad (4)$$

3. VOLTAGE ORIENTED CONTROL TECHNIQUE (VOC)

The voltage-oriented control (VOC) strategy is based on the knowledge of the position of the line voltage vector and the relative spatial orientation of the current vector. Typically, grid connected converters control-structures are based on Park's transformation to a rotating (*d-q*) reference frame (aligned with the line-voltage). In fact, it is usually built by two cascaded control loops so that a fast-inner loop controls the grid current and an external loop the DC-link voltage. The control structure of the proposed scheme is shown in Figure 1.

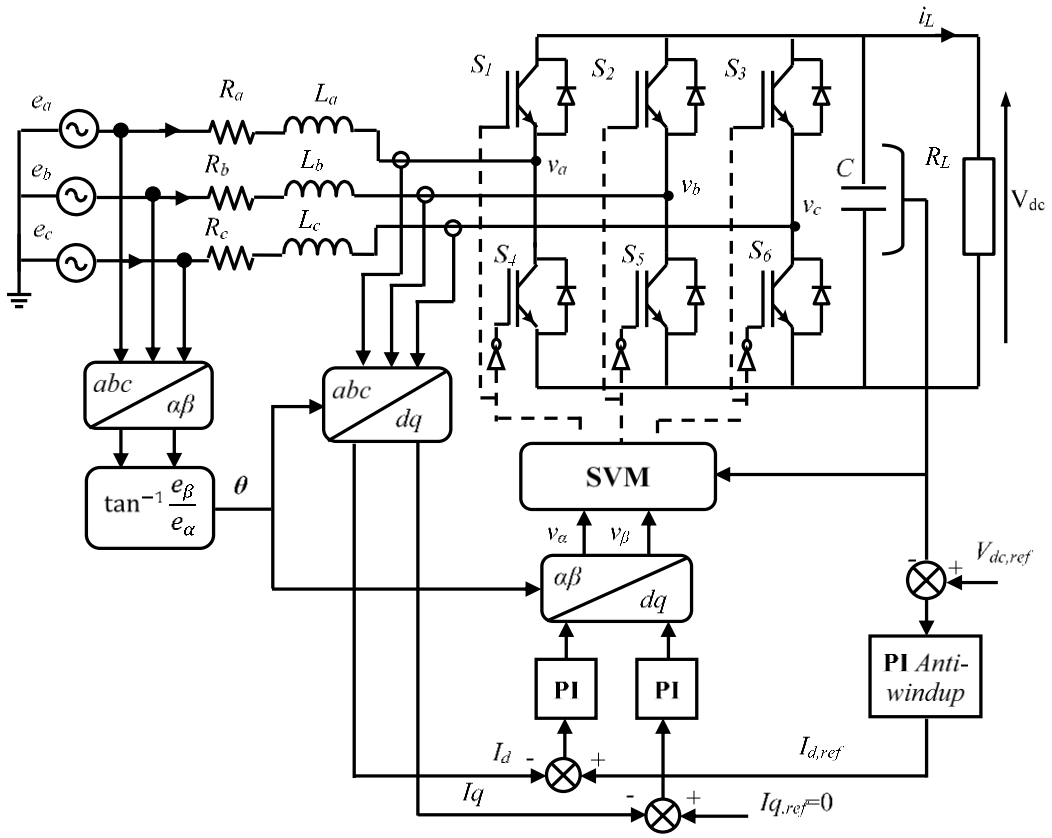

Figure 1. Structure of voltage oriented control in a rotating synchronous reference frame

It given in the synchronous (d-q) coordinates:

$$p = (e_q i_q + e_d i_d) = \frac{3}{2} E_m I_m$$
$$q = (e_q i_d - e_d i_q) \quad (5)$$

Different control strategies have been proposed for this three-phase boost operation [17], [18]. If i_q=0 and e_q=0 the active and reactive power equations will be simplified to $p = \frac{3}{2}E_m I_m$ and q=0. Based on these equations, the feedforward current control method is one of the widely used schemes for power control. Figure 3 shows the basic diagram of the controller. The *dq* current control and feedforward compensation are the main parts of this decoupled control scheme. The controller has an outer loop for the DC-bus voltage

regulation. This controller output sets the reference value for the *d* component of the current that controls the power [19].

– Current decoupling control of three-phase voltage source PWM rectifier

It is clear from (9) that the converter equations in the (d-q) axis are coupled to to each other through Lwi_q and Lwi_d terms, which means that if we control one of them, the other one will be changed correspondingly, thus we can not control them independently. So, we need to carry on the decoupling control in the order to control them independently. We use the strategy of feed-forward decoupling control, make:

$$\begin{cases} L\frac{di_d}{dt} + Ri_d = \left(k_p + \frac{k_i}{s}\right) * (i_{dref} - i_d) \\ L\frac{di_q}{dt} + Ri_q = \left(k_p + \frac{k_i}{s}\right) * (i_{qref} - i_q) \end{cases} \quad (6)$$

Substitute (6) into (5):

$$\begin{cases} v_d = \left(k_p + \frac{k_i}{s}\right) * (i_{dref} - i_d) - \omega L i_q + e_d \\ v_q = \left(k_p + \frac{k_i}{s}\right) * (i_{qref} - i_q) + \omega L i_d + e_q \end{cases} \quad (7)$$

Substitute (7) in (4):

$$\begin{cases} \frac{di_d}{dt} = \frac{1}{L}\left(k_p + \frac{k_i}{s}\right) * i_{dref} - \frac{1}{L}\left[R + (k_p + \frac{k_i}{s})\right] * i_d \\ \frac{di_q}{dt} = \frac{1}{L}\left(k_p + \frac{k_i}{s}\right) * i_{qref} - \frac{1}{L}\left[R + (k_p + \frac{k_i}{s})\right] * i_q \end{cases} \quad (8)$$

After decoupling control (8) we can control i_d and i_q independently, thus we can resperctively control the active and reactive powers independently and this can make de design of current loop mush easier. Current loop design block diagram is shown in Figure 3. In order to design the voltage loop, the reactive compoment be zero to insure the PWM rectifier uinity power factor [20]-[22]. The given value of active compenent i_d is produced by anti-windup PI controller, which shonw in (9), the k_p is the proportionly factor, the k_i is the integral coefficient.

$$i_{dref} = (k_p + \frac{k_i}{s})(V_{dc,ref} - V_{dc}) \quad (9)$$

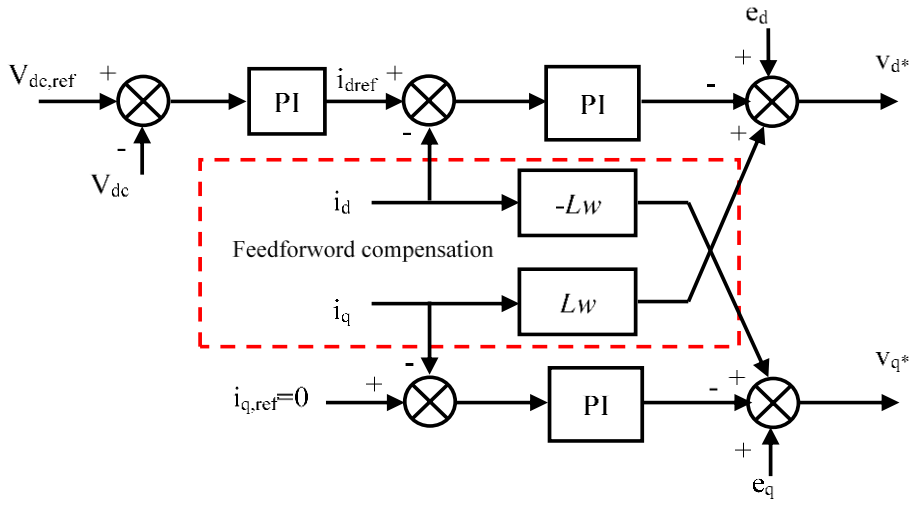

Figure 2. Structure diagram of currents decoupling

4. SYNTESIS OF CONTROLLERS

4.1. Design of current controller

The block diagram of current control loop is shown in Figure 4; basically, they tend to regulate the active and reactive current respectively. The *d*-axis current loop attempts to maintain a constant DC voltage by tracing the reference current value $i_{d,ref}$ produced by the outher voltage loop. In order to achieve the unity power condition, the *q*-axis current component $i_{q,ref}$ has to be set to zero [14].

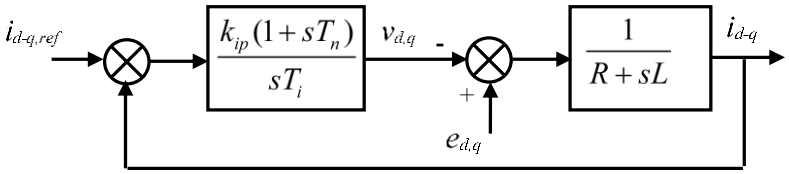

Figure 3. Current control loop diagram

The line voltage is seen as a constant perturbation, and is compensated by the integral part of PI controller. In this way, the zero of the PI controllers is placed over the pole of the system. So:

$$T_i = \frac{L}{R} \tag{10}$$

With this synthesis, in closed-loop, the system will be simplified and its closed loop transfer function is:

$$F(s) = \frac{1}{1+sT_iR} \tag{11}$$

The close-loop time constant $T_c = T_iR$ can be a specification of the controller design. So:

$$T_i = \frac{T_c}{R} \tag{12}$$

The parameters of the current loop PI controller can be given by:

$$k_{ip} = \frac{T_n}{T_i} = \frac{L}{T_c} \text{ and } k_{ii} = \frac{1}{T_i} = \frac{R}{T_c} \tag{13}$$

The active and reactive current control loops are similar; there-fore, the (13) is valid for both controllers.

4.2. Design of voltage controller

After correction, the current loop is considered to be equal to unity. Thus, the block diagram of voltage control loop is given in Figure 5. In order to limit DC bus voltage fluctuations a proportional-integral (PI) controller with anti-windup compensation is proposed for the DC bus regulation. The regulator acts using a proportional gain K_p, improving the dynamic and the quantity of intergrator via the gain K_i, for good operation in steady sate [23].

To limit the saturation of the output of the controller, caused by noise detection amplification, an anti-windup loop is added by a second integrator term, with a loop gain ($1/T_u$) chosen to high, without affecting the desired performances [24], [25]. Taking into account the PI regulateur function transfer function and that of the DC side, the synthesis of the K_p and K_i gains of the PI controller passes through placement of the poles of direct closed loop, is given by the following transfer function:

$$\frac{V_{dc}}{V_{dc,ref}} = \frac{k_p.s+k_i}{C.s^2+k_p.s+k_i} = \frac{k_p/C(s+k_i/k_p)}{s^2+k_p/C.s+k_i/C} \tag{14}$$

From (11), we note that the closed loop is a canonical transfer function of second order:

$$\frac{V_{dc}}{V_{dc,ref}} = \frac{\omega_n^2}{s^2+2.\xi.\omega_n.s+\omega_n} \tag{15}$$

By equalizing (14) and (15), and adopting an optimal damping coefficient; the gains of controller are quantified as follows:

$$k_p = 2.\xi.\omega_n.C \text{ and } k_i = C.\omega_n^2 \quad (16)$$

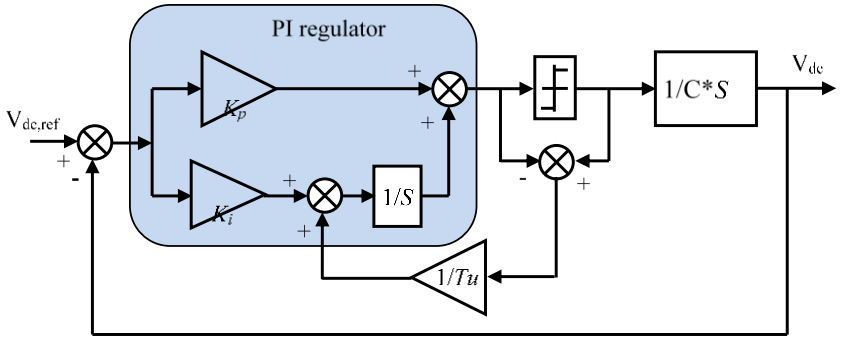

Figure 4. Anti-windup PI controller for DC-link voltage control

5. SPACE VECTOR MODULATION TECHNIQUE

The space vector modulation (SVM) is an alternative inverter switch control method to conventional sinusoidal PWM, it is characterized by a fast-transient response and a less harmonic distortion [26]. Control structure is greatly simplified and power electronic hardware is exploited to the maximum. The voltage vectors which are generated by the inverter for each sampling period are plotted in Figure 5. There are eight possible ouput voltage vectors, six active vectors V_1-V_6, and two zero vectors V_0-V_7 correspond to the inverter switches states S_0(000), S_1(100), …, S_7(111), respectively.

The principle of SVM is the prediction of inverter voltage vector by the projection of the reference between adjacent vectors in each sector N_i: $(i-1)\frac{\pi}{3} < S_i \leq i\frac{\pi}{3}$. The determination of the sector is based on the following expression:

$$\theta_s = arctan\left(\frac{V_{s\beta}}{V_{s\alpha}}\right) \quad (17)$$

where $V_{s\alpha}$ and $V_{s\beta}$ denote the voltage vector components in the Concordia reference.

The principle of the SVM's is to project the desired voltage vector Vs_{ref} on two adjacent voltage vectors V_i and V_{i+1} corresponding to two switching states of the inverter. The values of this projection provide the determination of desired commutation times T_i and T_{i+1} and correspond to two nonzero switching states of the inverter. To maintain the constant commutation frequency, in the case where $T_i+T_{i+1} \leq T_{PWM}$, a zero state of the inverter is applied during a complementary duration to the period T_{PWM}.

When the reference voltage vector V_{sref} is in sector 1 (Figure 5), it can compose by the active voltage vectors V_1, V_2 and V_0 [27], [28]. For a cycle switching, we have:

$$\vec{V}_{sref} = V_{s\alpha} + jV_{s\beta} = \frac{T_1}{T_{PWM}}\vec{V}_1 + \frac{T_2}{T_{PWM}}\vec{V}_2 \quad (18)$$

Where:

$$T_{PWM} = T_1 + T_2 + T_0 \quad (19)$$

The inclusion of zero basic vectors does'nt affect the vector sum V_{sref}, it only helps to balance the turn on and off periods of the transistors, and thus their power dissipation. The expressions of the voltage vector are:

$$\begin{cases} \vec{V}_1 = \sqrt{\frac{2}{3}}E(cos\,0 + j\,sin\,0) \\ \vec{V}_2 = \sqrt{\frac{2}{3}}E\left(cos\frac{\pi}{3} + j\,sin\frac{\pi}{3}\right) \end{cases} \quad (20)$$

The expression of T_1 and T_2 are as:

$$\begin{cases} T_1 = \left(\sqrt{\frac{3}{2}}V_{s\alpha} - \frac{1}{\sqrt{2}}V_{s\beta}\right).\frac{T_{PWM}}{E} \\ T_2 = \sqrt{2}V_{s\beta}\frac{T_{PWM}}{E} \end{cases} \quad (21)$$

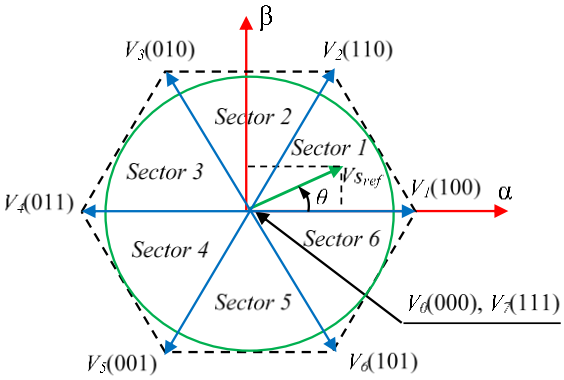

Figure 5. Principle of space vector modulation

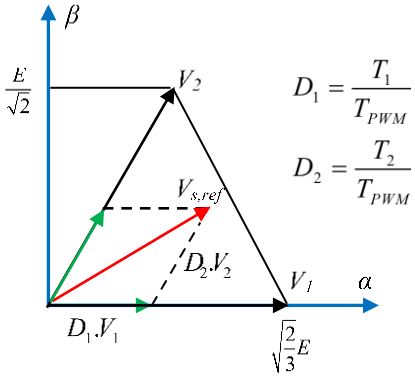

Figure 6. Projection of the reference voltage vector on V_1 and V_2

The equations for T_1 and T_2 are identically for all space vector modulation methods.

The only difference between the other types of SVM is the placement of zero vectors at the sampling time. The basic SVM method is the modulation method with symmetrical spacing zero vectors (SVPWM). In this method times T_0 and T_7 are equal [29]:

$$T_0 = T_7 = (T_{PWM} - T_1 - T_2)/2 \quad (22)$$

For the first sector switching sequence can be written as:

$$V_0 \rightarrow V_1 \rightarrow V_2 \rightarrow V_7 \rightarrow V_2 \rightarrow V_1 \rightarrow V_0 \quad (23)$$

6. SIMULATION AND EXPERIMENTAL RESULTS

In order to verify the effectiveness and the performance of the proposed control strategises, both simulation and experimental tests are carried out. Then a loratory setup was established using dSPACE system with DS1104 controller board and IGBTs voltage inverter. The electrical parameters of the power circuit and control data are listed in Table 1.

Table 1. System and control parameters

Prameter	Symbol	Value
AC line voltage (RMS)	e[V]	50
Frequency	f[Hz]	50
Line resistance	R[Ω]	0.2
Load resistance	R_L[Ω]	64
AC-side inductance	L[mH]	10
DC-bus capacitor	C[mF]	1.1
DC-bus voltage	V_{DC}[V]	125
Switching freqency	f_s[KHz]	10

6.1. Simulation results

Various tests, in simulation stadies, were conducted to verify performance of the proposed VOC scheme. The results shows the simulated waveforms under unity power factor (UPF) operation ($i_{q,ref}$=0) in the stady state for purely sinusoidal supply voltage source. Figures 7 (a)-(e) shows the dynamic behavior under a

step change of $V_{DC,ref}$, after a short transient, the output voltage is maintained close to its new reference. We remark that the anti-windup PI DC-bus controller has achived the test goals: no overshoots and better constancy in steady state. The line currents are very close to sine wave from with a spectral analysis devoid of low-order harmonics (*THD*=1.75%) and in phase with the power source voltage because the reactive current reference component $i_{q,ref}$ was imposed 0A. The reactive current (i_d) is maintained to zero.

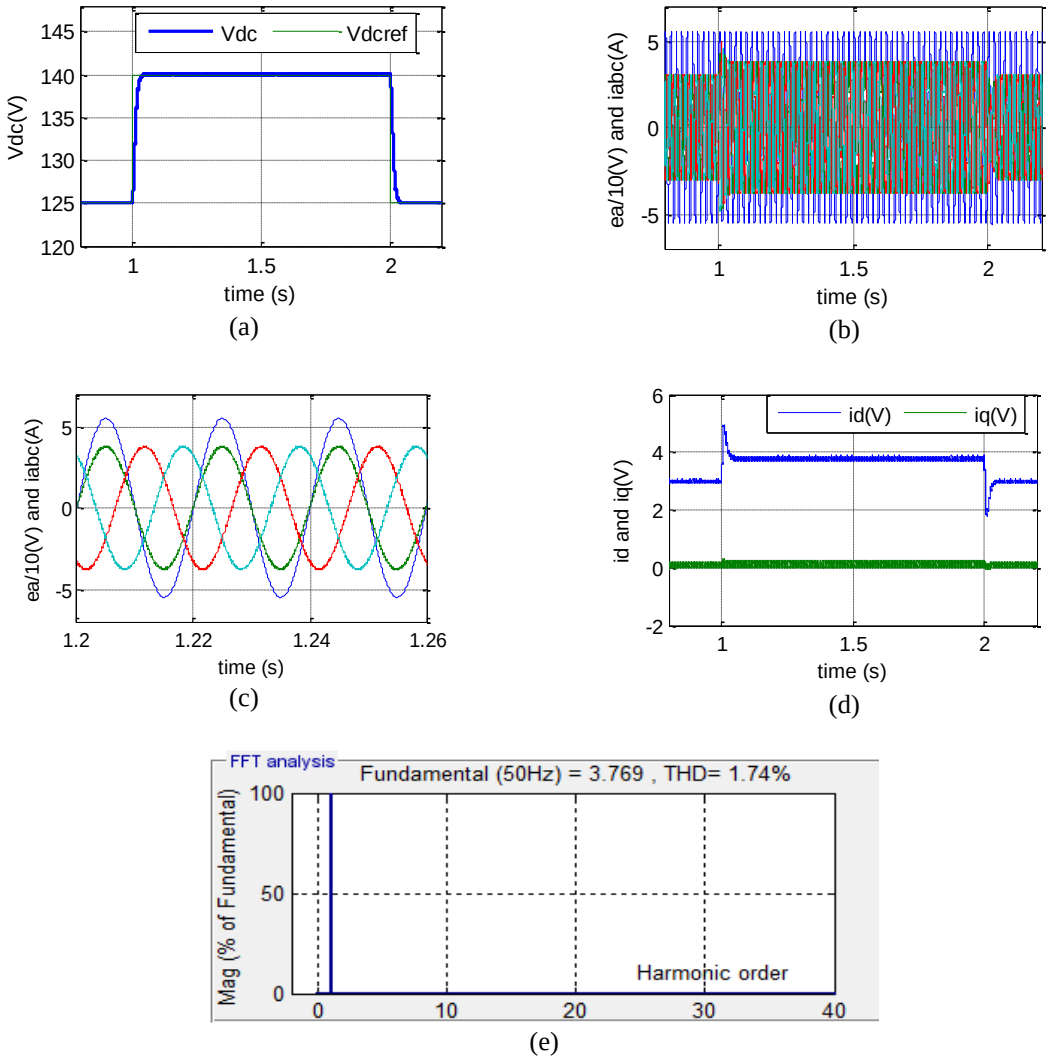

Figure 7. Dynamic response characteristics for step change of the $V_{DC\,ref}$, from 125V to 140V and inversely, using anti-windup PI controller, (a) DC-link voltage, (b) voltage e_a and currents phases, (c) zoom on voltage e_a and line currents, (d) dq-currents, (e) harmonic spectrum of line current

To show the good performance of the proposed VOC-SVM control based anti-windup PI controller during a transient, the load is changed in t_1=*1s*, from *64*Ω to *32*Ω. It is clearly shown in Figures 8 (a)-(d) that the system has a good dynamic response to variation load at *1s*. The current waveform is perfectely sinusoidal and has some phase as the voltage waveforms. The reactive current continued zero even with variation load. With anti-windup PI controller, the output voltage is recouvred in less than 0.05s.

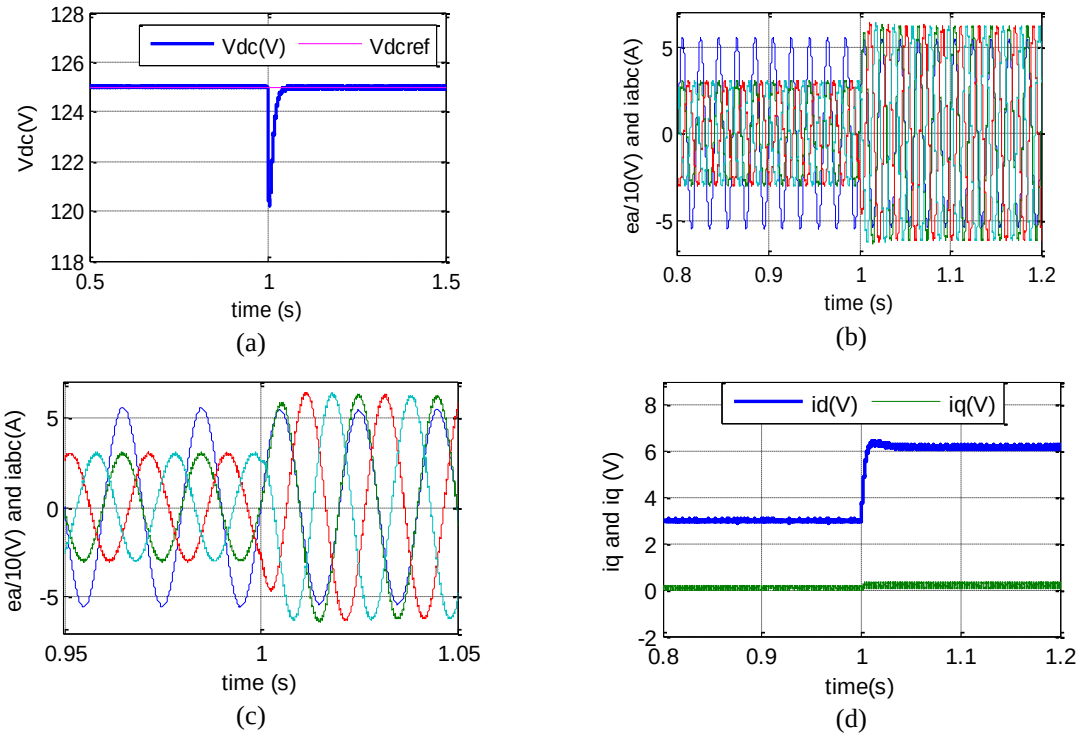

Figure 8. (a) DC-link voltage, (b)Voltage e_a and line currents, (c) zoom on voltage e_a and line currents, (d) dq-currents

6.2. Experimental results

To validate the simulation results of the proposed VOC-SVM with anti-windup PI controller studied on the above section, different pratical tests were carried out. An experimental test bench is designed by using a dSPACE 1104 board as illustrated in Figure 9. The dSPACE 1104 board is based on a 250MHz 603-Power PC-64 bits processor and a slave digital signal processing (DSP) card based on a 20MHz, TMS320F240-16bits microcontroller used to carry out real-time algorithms. The dSPACE works on MATLAB/Simulink R2013b platform. The board is equibed with analog-digital converter for voltages and currents sensors; it's used with control desk software which makes the record of the results easy.

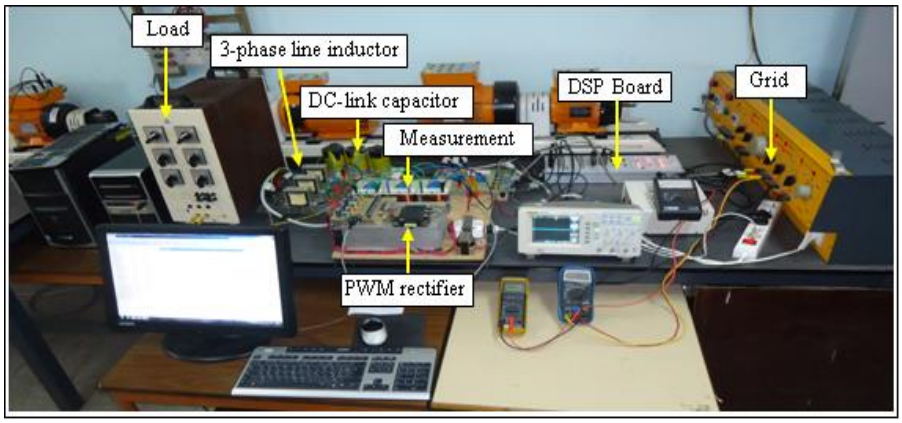

Figure 9. Different parts of experimental test bench and its dSPACE control

Loking at the experimental results, we can see the dynamic of the VOC-SVM under a step change of V_{DCref} is presented in Figures 10 (a)-(e), after ashort transient the DC-bus voltage is maintained close to its

new reference with good dynamic, stability and no overshoots. The line current i_a shown in Figure 10 (c) is in phase with the actual power source voltage because the reactive current is controlled to zero, that ensures unity power factor operation. From the Figure 10 (d), it can be found that the active current control and the reacrive current control are independent of each other.

The robustness of this control is proven by the exprerimental results of a step response during a variation of the load (Figures 11 (a)-(e)), the grid currents rmains purely sinusoidal and unaffected by this load variation. Furthmore, it can be seen that the DC-bus voltage, active current and reactive current remains regulated at its reference value after a short transient of 50ms. In addition, it is also seen that the active current undergoes a relative increase in this load variation. The quadrature current i_q is kept zero (Figure 11 (d).

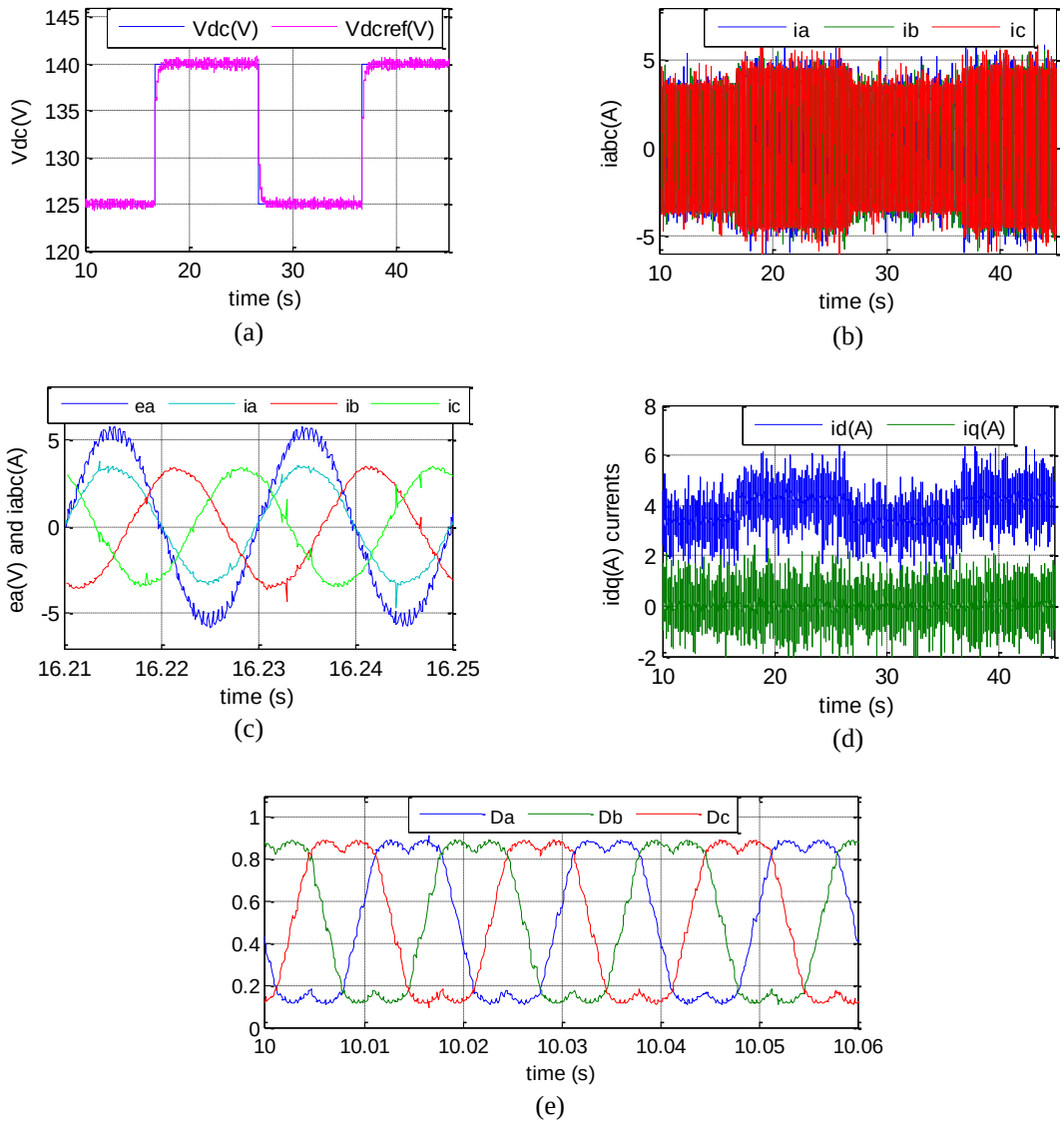

Figure 10. Experimental results of, (a) DC-bus voltage, (b) line currents, (c) zoom on voltage and line currents, (d) dq-currents, (e) duty cycle ratio of SVPWM based on the carrier. Transient response during a step change of V_{DCref} from 125V to 140V and inversely

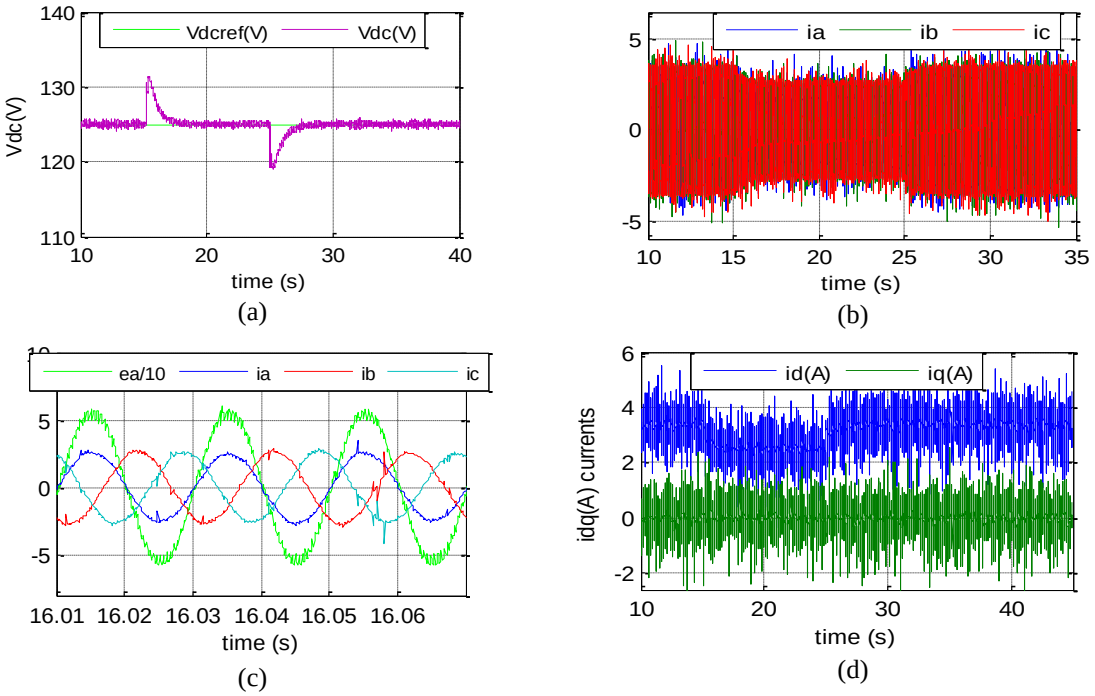

Figure 11. Experimental results of (a) DC-bus voltage, (b) line currents, (c) a focused part of voltage and line currents, (d) dq-curents transient response during a load change, from *64*Ω to *86*Ω and inversel

7. CONCLUSION

In this paper, simulation and real time implementation study of VOC-SVM control of three phase PWM rectifier combined with a anti-windup PI controller of DC-bus voltage is presented. For this purpose, simulation and experimental results shows that the proposed control is able to garantees a good regulation of the output voltage and give a perfectly sinusoidal line current with a good THD that meets IEEE-519 (THD<2%). In addition, the decoupled feed-forward control strategies ensure a fast-dynamic response and very good decoupling in active and reactive current control. On the other hand, the proposed VOC scheme operates with the symetrical SVM that are offering better DC-bus voltage utilization, lower switching loss and a constant switching frequency.

REFERENCES

[1] J. R. Rodríguez, L. Dixon, JR. Espinoza, J. Pontt, and P. Lezana, "PWM regenerative rectifiers : state of the art," *IEEE Transactions on Industrial Electronics*, vol. 52, no. 1, pp. 5-22, Feb. 2005, doi: 10.1109/TIE.2004.841149.

[2] J. A. A. Caseiro, and A. M. S. Mends, "Performance analysis of three-phase PWM rectifiers for high power quality applications," in *International Conference on Renewable Energies and Power Quality (ICREPQ'09)*, Valencia, Spain. 2009, doi: 10.24084/repqj07.388

[3] J. W. Wilson, "The forced commutated inverter as a regenerative rectifier," *IEEE Transactions on Industry Applications*, vol. IA-14, no. 4, pp. 335-340, July 1978, doi: 10.1109/TIA.1978.4503547.

[4] S. Hansen, M. Malinowski, F. Blaabjerg, and M. P. Kazmierkowski, "Sensorless control strategies for PWM rectifier," in *APEC 2000. Fifteenth Annual IEEE Applied Power Electronics Conference and Exposition (Cat. No.00CH37058)*, 2000, pp. 832-838 vol.2, doi: 10.1109/APEC.2000.822601.

[5] C. J. Zhan, Y. Han, T, Xie, Z. Y. Zhao, and M. C. Wong, "Mathematical model and dual-DSP control of tri-level PWM reversible rectifier," in *Proceedings of the IEEE 1999 International Conference on Power Electronics and Drive Systems. PEDS'99 (Cat. No.99TH8475)*, 1999, pp. 174-179 vol.1, doi: 10.1109/PEDS.1999.794556.

[6] M. P. Kazmierkowski, and L. Malesani, "Current control techniques for three-phase voltage-source PWM converters: a survey," *IEEE Transactions on Industrial Electronics*, vol. 45, no. 5, pp. 691-703, Oct. 1998, doi: 10.1109/41.720325.

[7] Y. Ye, M. Kazerani, and V. H. Quintana, "A novel modeling and control method for three-phase PWM converters," in *2001 IEEE 32nd Annual Power Electronics Specialists Conference (IEEE Cat. No.01CH37230)*, 2001, pp. 102-107 vol. 1, doi: 10.1109/PESC.2001.954002.

[8] T. Noguchi, H. Tomiki, and S. Kondo, "Direct power control of PWM converter without power-source voltage sensor," *IEEE Transactions on Industry Applications*, vol. 34, no. 3, pp. 473-479, May-June 1998, doi: 10.1109/28.673716.
[9] A. Bouafia, F. Krim, and J. P. Gaubert, "Fuzzy-logic-based switching state selection for direct power control of three-phase PWM rectifier," *IEEE Transactions on Industrial Electronics*, vol. 56, no. 6, pp. 1984-1992, June 2009, doi: 10.1109/TIE.2009.2014746.
[10] M. Liserre, A. Dell'Aquila, and F. Blaabjerg, "An overview of three-phase voltage source active rectifiers interfacing the utility," in *2003 IEEE Bologna Power Tech Conference Proceedings*, 2003, pp. 8 pp. Vol.3, doi: 10.1109/PTC.2003.1304405.
[11] A. M. Razali, and M. A. Rahman, "Performance analysis of three-phase PWM rectifier using direct power control," in *2011 IEEE International Electric Machines & Drives Conference (IEMDC)*, 2011, pp. 1603-1608, doi: 10.1109/IEMDC.2011.5994600.
[12] M. Cichowlas, and M. P. Kamierkowski, "Comparison of current control techniques for PWM rectifiers," in *Industrial Electronics, 2002. ISIE 2002. Proceedings of the 2002 IEEE International Symposium on*, 2002, pp. 1259-1263 vol.4, doi: 10.1109/ISIE.2002.1025970.
[13] M. Malinowski, M. P. Kazmierkowski, and A. Trzynadlowski, "Review and comparative study of control techniques for three-phase PWM rectifiers," *Mathematics and Computers in Simulation*, vol. 63, pp. 349–361, 2003, doi: 10.1016/S0378-4754(03)00081-8.
[14] A. M. Hava, R. J. Kerkman, and T. A. Lipo, "A high performance generalized discontinuous PWM algorithm," in *Proceedings of APEC 97-Applied Power Electronics Conference*, 1997, pp. 886-894 vol. 2, doi: 10.1109/APEC.1997.575750.
[15] W. Jiuhe, Y. Hongren, Z. Jinlong, and Li Huade, "Study on power decoupling control of three phase voltage source PWM rectifiers," in *2006 CES/IEEE 5th International Power Electronics and Motion Control Conference*, 2006, pp. 1-5, doi: 10.1109/IPEMC.2006.4778015.
[16] C.T. Pan, and C.T. Chen "Modeling and analysis of a three-phase PWM AC-DC converter without current sensor," in *IEE Proceedings B (Electric Power Applications)*, vol. 40, March 1993, doi: 10.1049/ip-b.1993.0024.
[17] J. Lamterkati, M. Khafallah, L. Ouboubker, A. Elafia, and H. Chaikhy, "Implementation of voltage-oriented control of three-phase PWM rectifier, via Fuzzy and PI controller for output voltage regulation," *Journal Engineering and applied Sciences JEAS, Medwell Journals*, vol. 13, no: 14, pp.5756-5763, september, 2018, doi: 10.36478/jeasci.2018.5756.5763.
[18] M. Malinowski, "Sensorless control strategies for three-phase pwm rectifiers", Ph.D. dissertation, Faculty of Electrical Engineering, Institute of Control and Industrial Electronics, Warsaw University of Technology, 2001.
[19] J. F. Mandiola, D.C. Carmona, S. Haghbin, T. Abdulahovic, and M. Ellsen, "An FPGA Implementation of a Voltage-Oriented Controlled Three-Phase PWM Boost Rectifier," in *2012 Electrical Systems for Aircraft, Railway and Ship Propulsion*, 2012, pp. 1-6, doi: 10.1109/ESARS.2012.6387430.
[20] B.R. Lin, H.H. Lu, and Y.L. Huo, "Single-phase power factor correction circuit with three-level boost converter," in *ISIE '99. Proceedings of the IEEE International Symposium on Industrial Electronics (Cat. No.99TH8465)*, 1999, pp. 445-450 vol.2, doi: 10.1109/ISIE.1999.798653.
[21] P. C. Loh, M. J. Newman, D. N. Zmood, and D. G. Holmes, "Improved transient and steady state voltage regulation for single and three phase uninterruptible power supplies," in *2001 IEEE 32nd Annual Power Electronics Specialists Conference (IEEE Cat. No.01CH37230)*, 2001, pp. 498-503 vol.2, doi: 10.1109/PESC.2001.954163.
[22] D. Zmood, D. Holmes, and G. Bode, "Frequency-domain analysis of three-phase linear current regulators," *IEEE Transactions on Industry Applications*, vol. 37, no. 2, pp. 601-610, March-April 2001, doi: 10.1109/28.913727.
[23] X.-l. Li, J.-G. Park, and H.-B. Shin, "Comparison and evaluation of anti-Windup PI Controller," *Journal of Power Electronics*, vol. 11, issue. 1, pp. 45-50, 2011, DOI:10.6113/JPE.2011.11.1.045.
[24] S. Ouchen, J. Gaubert, H. Steinhart, and A. Betka, "Energy quality improvement of three-phase shunt active power filter under different voltage conditions based on predictive direct power control with disturbance rejection principle," *Mathematics and Computers in Simulation*, vol. 159, pp. 506-519, 2019, doi: 10.1016/j.matcom.2018.11.024.
[25] S. Saidi, R. Abbassi, and S. Chebbi, "Virtual fux based direct power control of shunt active filter, "*Computer Science & Engineering and Electrical Engineering*, vol. 21, issue. 6, pp. 2165-2176, 2014.
[26] K. Zhou, and D. Wang, "Relationship between space-vector modulation and three-phase carrier-based PWM: a comprehensive analysis [three-phase inverters]," *IEEE Transactions on Industrial Electronics*, vol. 49, no. 1, pp. 186-196, Feb. 2002, doi: 10.1109/41.982262.
[27] A. El afia, M. Khafallah, A. Chériti, B. Elmoussaoui, and A Saad, "A Simple Direct Torque Fuzzy Control of Induction Motor Using Space Vector Modulation," *European Power Electronics and Drives* (*EPE Journal)*, vol. 5, pp. 25-30, 2005, doi: 10.1080/09398368.2005.11463586.
[28] A. Ouarda, and F. Ben Salem, "Induction machine DTC-SVM: A comparison between two approaches," in *10th International Multi-Conferences on Systems, Signals & Devices 2013 (SSD13)*, 2013, pp. 1-7, doi: 10.1109/SSD.2013.6564091.